

257

5/26/94

E8167

PSIDD: A Post-Scan Interactive Data Display System for Ultrasonic Scans

Don J. Roth and Steven A. Szatmary

November 1993



PSIDD: A Post-Scan Interactive Data Display System for Ultrasonic Scans

Don J. Roth
Lewis Research Center
Cleveland, Ohio

and

Steven A. Szatmary
Cleveland State University
Cleveland, Ohio



Office of Management

Scientific and Technical
Information Division

1993

Summary

An ultrasonic data display system was developed at NASA Lewis Research Center that allows the user to interactively examine digitized waveforms and processed information associated with any specific scan location of an ultrasonic contact scan. This information is displayed on a video display monitor and includes acquired time-domain waveforms, frequency-domain magnitude and phase spectra, and ultrasonic properties (pulse velocity, phase velocity, reflection coefficient, attenuation coefficient, attenuation coefficient error) as a function of frequency for a material. This report describes the system features and illustrates the system's usefulness for nondestructive materials characterization.

I. Purpose of PSIDD System

The post-scan interactive data display system (PSIDD) has been developed for viewing raw (digitized) data and resulting properties at any scan location on any of the ultrasonic images formed from ultrasonic contact scans.¹ It was developed to (1) confirm the accuracy of images both from a software signal processing and hardware performance standpoint and (2) interactively compare ultrasonic properties at different locations within samples. In ultrasonic contact scanning, two front surface and two back surface ultrasonic pulses obtained using the pulse-echo configuration are digitized and stored at every scan location. Subsequently, the pulses associated with each scan point are Fourier-transformed to the frequency domain and used in calculating ultrasonic reflection coefficient, attenuation coefficient, cross-correlation (pulse) velocity, and phase velocity (fig. 1).¹ Images of these ultrasonic properties are then formed at preselected frequencies. This ultrasonic method is especially sensitive for quantifying global variations (such as pore fraction variations) in microstructure¹ as well as detecting isolated material defects² in monolithic and composite materials. Microstructural variations are indicated via gray or color scale variations in an ultrasonic image; at such locations there can be questions as to the validity of the indication. PSIDD allows the operator to examine the digitized ultrasonic waveforms at such locations and verify whether the waveforms and the resulting ultrasonic properties are valid, and, if valid, how the waveforms and properties differ from those at other sample areas. This form of analysis is likely to yield more accurate

predictions of material behavior, and it can be the basis for artificial intelligence techniques that allow defect identification based on waveform shapes and property versus frequency behavior. This type of comprehensive analysis in such a convenient format is not commonly done in conventional ultrasonic testing.

II. System Overview

a. Hardware and Software

The system uses a VAX 4000 - 200 computer running VAX/VMS A5.5-1 operating system interfaced to a Grinnell 274 image processing system via a DRV11 direct memory access board installed on the VAX's Q-bus. Two video displays are used (fig. 2(a)). A DEC VT340 terminal is the user terminal attached to the computer and a Mitsubishi 20LP is the video display monitor attached to the image processing system. A cursor control unit is attached to the image processor. High-level VAX FORTRAN software used for driving the system was written at the Lewis Research Center. The Grinnell library of FORTRAN subroutines³ is called from this high-level software. The user starts the PSIDD program and is queried from the user terminal. The video display monitor shows ultrasonic images and the associated waveforms, spectra, and properties.

b. User Interface

The PSIDD user interface consists of the VT340 user terminal, the 20LP video display, the cursor control unit (CCU), and the PSIDD executable code. PSIDD is started from the user terminal after logging into an account on the VAX. The user terminal is used to query the initial user options and display error messages. The video display monitor is used in conjunction with the CCU to display image and waveform information. Three different display screens are shown on the video display during PSIDD operation: (1) image display, (2) waveform display, and (3) graph display. The image display is used to view the ultrasonic property images and to select scan locations where the user wishes to examine the digitized waveforms, spectra, and frequency-dependent property data. The waveform display is the screen that actually displays this information, and the graph display is a full screen enlargement of one

of the graphs from the waveform display. The movement of the CCU joystick and the positioning of the function switches on the CCU cause PSIDD to switch among the three screens and perform different tasks depending on which screen is currently displayed on the video display.

c. Features For Application to Ultrasonic Contact Scan Images

PSIDD first allows the display of any of the ultrasonic property images at predetermined frequencies generated from spectral analysis of ultrasonic contact scan data. These images include cross-correlation (pulse) velocity, phase velocity, reflection coefficient, attenuation coefficient, and attenuation coefficient error.¹ From a grid overlaying the image and representing the locations where ultrasonic data were obtained, and the use of the CCU, PSIDD allows the operator to examine time-domain waveforms at any location where ultrasonic data were obtained. PSIDD also allows the user to examine at these locations (1) the frequency-domain magnitude and phase spectra of the waveforms and (2) the calculated ultrasonic material properties including phase velocity, reflection coefficient, attenuation coefficient, and attenuation coefficient error as a function of frequency. Digitized and calculated property data obtained from an ultrasonic contact scan and stored in files are retrieved via a direct access data retrieval algorithm which allows display of data at any point. All this information is displayed on the video display. For the frequency-domain transformed waveforms and frequency-dependent properties portions of the video display, the user can move the CCU over any waveform box to view on video in real-time specific values of waveforms and properties at any frequency within the broadband frequency regime realized during the ultrasonic contact scan. Waveforms are auto-scaled in both horizontal and vertical directions and can be individually enlarged to take up the entire video display for more detailed viewing. The user can choose to view the two back surface waveforms with or without the ultrasonic system noise subtracted. Where interpolation of spectra and property data is needed, the user has the choice of linear or natural cubic spline interpolation.

III. Detailed Explanation of PSIDD Operation and Features

a. Initial Setup and Queries

Before using PSIDD, the user is first required to edit an initialization file (PSIDD.ini) that tells PSIDD in which file directory path the image and data files generated from the ultrasonic contact scan are located. The user then runs PSIDD by typing "run PSIDD" at the DCL (Digital Command Language) prompt on the user terminal and is queried regarding data set prefix name. In this example, a scanned silicon nitride sample having scan information stored in files with file name

prefix SN2_CC_10 is confirmed and PSIDD displays messages to the user terminal regarding the files read in associated with this prefix (fig. 2(b)). The user is then asked what specific image type and frequency are desired (fig. 2(c)). Here, as an example, phase velocity is chosen for the image type and 60 MHz is chosen for the frequency. At this point, the image display comes up to video with a grid overlaying the image that represents the locations where ultrasonic data were obtained (fig. 3(a)). As will be explained, the image can be viewed without the grid if a clearer view is necessary (fig. 3(b)). In figure 3(a), the outlying black areas overlayed with the grid represent areas of the rectangular holder which contained the disk-shaped sample. A scale marker is present in the lower right corner below the gray scale bar. The 60-MHz phase velocity image indicates material gradients via gray scale variations. These gradients will be investigated with PSIDD in section IV.

Figure 4 shows the CCU attached to the image processing system that allows options to be executed for the PSIDD system. Figures 5(a) to (c) show the menus to be used in conjunction with the CCU for selecting options in the **image display**, **waveform display**, and **graph display**, respectively. The CCU has two switches labeled "FUN A" and "FUN B." All the options on the three menus are accessed by moving the cursor control joystick, toggling the FUN A and FUN B switches (down = 0 and up = 1), and, subsequently, pressing the ENTER button on the CCU. (For the image processor setup used at Lewis Research Center, the cursor 1 switch on the CCU must be in the "up" position to allow cursor viewing.) With FUN A = 0 and FUN B = 0, by depressing the "Q" key on the user terminal keyboard and the enter key on the CCU, the user can quit PSIDD at any point in the program.

b. Image Display

For the image display, the following four options exist as shown in the **image display** menu (fig. 5(a)). With FUN A = 0 and FUN B = 1, the image color scheme can be varied from gray scale to a variety of different color schemes, two of which are shown in figures 6(a) and (b). With FUN A = 1 and FUN B = 0, locations where ultrasonic scan data and resulting property values are deemed questionable (from analysis performed after the contact scan) are highlighted as shown in figure 7. Each different color and pattern scheme represents a different questionable data condition and indicates what ultrasonic property might be affected. Codes BA, BC, BP, and BV represent locations where attenuation coefficient, cross-correlation velocity, phase velocity, and both types of velocities, respectively, might be suspect as a result of faulty data. Code BE represents edge locations for a nonrectangular sample. Table I gives the criteria used to code the potentially suspect scan locations.

As explained in the following paragraphs, the highlighting allows the user to (1) go to highlighted locations for a closer examination of the digitized and processed data and (2) perform data filtering as needed to obtain a more accurate image if the

data are deemed bad. With FUN A = 1 and FUN B = 1, the user terminal displays the queries shown in figure 2(b) and the user has the opportunity to select a new image type. With the video cursor moved to a specific image location ($x = 11$, $y = 12$) (displayed in the upper right corner of figs. 8(a) and (c)), and FUN A = 0 and FUN B = 0, the waveform data corresponding to the cursor location on the image is displayed on video figs. 8(b) and (d)). If the cursor is not on the image grid area and FUN A = 0 and FUN B = 0, then the overlaid image grid is toggled off and on.

c. Waveform Display

The waveform display shown in figure 8(b) has 13 boxes of information associated with the scan point. The top row of boxes show digitized time-domain ultrasonic waveform data from the pulse-echo ultrasonic contact measurement (fig. 1) at that location. In figure 8(b) the waveforms labeled FS1(T) and FS2(T) are the first front surface reflections without and with the sample present on the buffer rod, respectively, where T is time. The waveforms labeled B1(T) and B2(T) are the first and second ultrasonic pulses reflected off the sample back surface. The delay times relative to the main ultrasonic pulse where the echoes occur are given at the top of the four boxes. The time and voltage scales of the waveforms are shown in the lower right and middle left of the boxes, respectively. The time scale is denoted by a scale marker, and the voltage scale is given in volts (V)/division (D).

The middle four boxes of the waveform display in figure 8(b) show ultrasonic properties as a function of frequency. The equations used to calculate frequency-dependent ultrasonic properties obtained from the pulse-echo configuration are given in the appendix. The first box on the left shows the Fourier-transformed front surface reflections FS1(F) and FS2(F) magnitude spectra where F is frequency. The spectra are color coded. Highest magnitude in volt-sec is shown at the upper left, and frequency scale (auto-scaled based on frequency extent of magnitude spectra) is shown at the middle right. The selected image frequency of 60 MHz is pointed at with a dotted line. The next two boxes to the immediate right show phase angle (θ) and magnitude spectras for Fourier-transformed back surface reflections B1(F) and B2(F). The lower left of the phase angle spectra box shows the lowest phase angle (referenced from $\theta = 0^\circ$) in terms of number of 360° revolutions (RV) plus the number of degrees less than 360° . (Please note that the number of revolutions can be a function of the signal processing routine's attempt to provide a continuous curve for phase angle vs. frequency.) A dotted line in the magnitude spectra box points to the ratio of the B1(F) and B2(F) magnitudes at the selected image frequency of 60 MHz. As before, highest magnitude in volt-sec is shown at the upper left of the magnitude spectra box and frequency scaling (which is the same as for the FS1(F)/FS2(F) box) is displayed at the middle right of both boxes. The next box to the right contains two graphs: the upper one contains phase velocity (cm/ μ sec) as a function of fre-

quency while the lower one shows the ratio of phase velocity to cross-correlation velocity as a function of frequency. The next box to the right displays reflection coefficient as a function of frequency. As before, the magnitudes of the properties at the selected image frequency are pointed at with a dotted line and displayed.

The lowest set of boxes shows attenuation coefficient as a function of frequency (neper (NP)/cm (CM)) (left-most box), % error in the attenuation coefficient as a function of frequency (middle), and an information box (right-most box). The attenuation coefficient box shows color-coded error (\pm sigma) bands which were derived from the % error in the attenuation coefficient calculation. The error bands and % error in attenuation coefficient are necessary to show what frequencies are most valid for the attenuation coefficient calculation. The information box displays the present date, sample name, sample thickness, scan position, nominal transducer center frequency, cross-correlation velocity, phase velocity at the selected image frequency, frequency range over which extreme-value data filtering/clipping was performed, and whether the scan location is "good" (G) or "potentially bad" (BA, BC, BP, BV, or BE) where "potentially bad" refers to the questionable data previously discussed.

At this point, movement of the video cursor into the lower two rows of boxes on the waveform display allows the display of ultrasonic property values at any frequency in the lower right corner of the information box (fig. 8(e)). In figures 8(e) and (f), phase velocity at 78 MHz and the ratio of B1(F)/B2(F) at 65 MHz are displayed, respectively, by moving the video cursor into the appropriate boxes. With the waveform display on video, the following four options exist as shown in the **waveform display** menu (fig. 5(b)). With FUN A = 0 and FUN B = 0, the user is returned to the image display. With FUN A = 0 and FUN B = 1, the waveform display can be toggled between color and gray scale schemes (fig. 8(g)). The gray scale scheme can be used if a gray scale printer is available or gray scale hardcopies are required. With FUN A = 1 and FUN B = 0, and the cursor located in one of the two back surface echo (B1(T) or B2(T)) boxes in the top row of boxes, the specific waveform can be displayed with or without noise subtracted. (Noise at the time delays where the back surface echoes were located was digitized and stored before the couplant and sample were placed on the ultrasonic transducer.) The bottom text line in the information box will now show if the waveform is displayed with or without noise subtracted (fig. 8(h)). With FUN A = 1 and FUN B = 1, the B2(T) box can now be enlarged for a closer examination if necessary (fig. 9(a)). With FUN A = 1 and FUN B = 0, and the cursor located in one of the lower two rows of boxes showing ultrasonic properties as a function of frequency, the graph interpolation method can be toggled from spline to linear. The bottom (small) text line in the information box will now show if the waveform is displayed using linear or spline interpolation (fig. 8(e)). Spline interpolation provides smoothed graphs in comparison to those displayed with linear interpolation and is useful when ultrasonic

contact scans have been performed at nominal frequencies less than ~20 MHz. Linear interpolation is a speedier algorithm and results in only slightly less smooth graphs when ultrasonic contact scans have been performed at nominal frequencies greater than ~20 MHz. With FUN A = 1 and FUN B = 1, the phase velocity versus frequency box can now be enlarged for a closer examination if necessary (fig. 9(b)).

d. Graph Display

The enlarged graph displays allow more detailed examination of waveforms and frequency-dependent properties. In the graph displays showing ultrasonic properties versus frequency, movement of the video cursor allows the display of ultrasonic property values at any frequency (within the broadband frequency regime realized during the ultrasonic contact scan) in the lower right corner of the screen (fig. 9(c)). The **graph display** menu applies to these enlarged full-screen displays of one of the graphs on the waveform display, and the following four options exist. With FUN A = 0 and FUN B = 0, the user is returned to the waveform display. With FUN A = 0 and FUN B = 1, the user can toggle the enlarged image between color and gray scale. If FUN A = 1 and FUN B = 0, and the graph displayed is one of the two back surface echoes, the noise subtraction option can be toggled. If FUN A = 1 and FUN B = 0, and the graph displayed is one of the ultrasonic property versus frequency plots, then the interpolation method is toggled between linear and spline. If FUN A = 1 and FUN B = 1, and the graph displayed is one of the two back surface echoes, the waveform is displayed with and without the noise subtracted (fig. 9(d)). If FUN A = 1 and FUN B = 1, and the graph displayed is one of the ultrasonic property versus frequency plots, the plot is displayed with both interpolation options (fig. 9(e)).

IV. Examples of Application to Materials Characterization Research at Lewis

Two examples are presented here showing the usefulness of this system for nondestructive materials characterization. The examples show post-scan analyses of a silicon nitride disk sample scanned with a 125-MHz broadband ultrasonic transducer and a ceramic matrix composite (SiC fiber/Calcium-Alumina-Silica matrix) plate sample scanned with a 10-MHz broadband ultrasonic transducer, respectively.

a. Examination of waveforms and frequency-dependent properties at different regions of silicon nitride disk

As shown in the previous section, the 60-MHz phase velocity image of the silicon nitride disk indicates material gradients via gray scale variations (fig. 3). Specifically, six circular areas of very dark shading (low velocity), a moderately dark central region (average to slightly below average velocity), and a light

edge (high velocity) are shown. Through destructive methods, these regions were shown to differ in pore fraction.¹ The origin of the differences between the different colored regions (figs. 8(a) and (c)) can be explored in terms of ultrasonic properties by examining the waveforms and properties. For example, examining the phase angle graphs of the different regions on the waveform displays (figs. 8(b) and (d)) shows that over the same frequency range the phase angle spread ($\Delta\theta$) is greater at the dark spot than at the light edge region. This leads to the differences in the phase velocity for the different regions of the disk (a greater $\Delta\theta$ results in a lower phase velocity), thus verifying the validity of the image. Moving the video cursor in the respective phase velocity boxes and comparing velocity values show the trend of lower velocity at the dark spot for all frequencies. Also, if the back surface echoes B1(T) and B2(T) in figs. 8(b) and (d) are compared, the waveforms in figure 8(b) corresponding to the low velocity location of the disk are shifted to the right (out in time; B2(T) is most noticeably shifted) in the respective time windows in relation to those in figure 8(d) corresponding to the high velocity edge location. Thus, observed cross-correlation (pulse) velocity differences between the two regions are verified by examining the digitized waveforms (see respective information boxes at lower right of waveform displays).

It is instructive to look at the attenuation coefficient image at 60 MHz of the same sample. When the new image type option on the **image display** (FUN A = 1 and FUN B = 1) menu is used, the attenuation coefficient image at 60 MHz is displayed to video (fig. 10(a)). Comparing this image with the phase velocity image (fig. 3) shows that sample positions where *changes* in velocity with position (i.e., material gradients) were most severe corresponded to areas of highest attenuation coefficient. Examining waveform displays at high and low attenuation coefficient locations (figs. 10(b) to (e)) reveals interesting contrasts. The B2(T) waveform at the high attenuation coefficient location is lower in amplitude and distorted when compared to the B2(T) waveform at the low attenuation coefficient location. This contrast also manifests itself in the B2(F) magnitude graphs. The B2(F) graph at the high attenuation coefficient location shows a double-peak characteristic (causing the location to be designated BA [see information box and fig. 7]) with a severe dropout in the 60-MHz region as compared to that for the low attenuation coefficient region. Comparing attenuation coefficient versus frequency behavior shows that (1) the attenuation coefficient at 60 MHz is more than an order of magnitude greater at the high attenuation coefficient location than at the low attenuation coefficient location (both have a calculated error of ~50%) verifying the validity of the image and (2) the attenuation coefficient versus frequency slope is much greater at the high attenuation coefficient location than at the low attenuation coefficient location in the ~30 to 60 MHz frequency range. (In this frequency range, the calculated error in the attenuation coefficient is on the order of $\leq 50\%$.) The phase velocity versus frequency behaviors over the frequency

range 10 to 130 MHz also show differences at the two locations. Both locations show phase velocity decreasing with frequency but the higher attenuation coefficient location shows a greater velocity decrease (from ~ 1.12 to 1.07 cm/ μ sec) and steeper velocity versus frequency slope than does the low attenuation coefficient location (which shows a velocity decrease from ~ 1.09 to 1.08 cm/ μ sec). The latter result indicates that sharp material *gradients* also affect phase velocity behavior. (Closer examination of these differences between locations can be accomplished by using the graph enlarge option [FUN A = 1 and FUN B = 1] on the **waveform display** menu.) It is envisioned that different subsurface defect conditions (pore vs. inclusion) would generate characteristic signatures that could be identified through the combination of waveform shape and ultrasonic property versus frequency behavior.

Figure 7 shows a number of scan locations coded BA including location $x = 34, y = 9$ (fig. 11(a)). At this point, the waveform display shows an improperly digitized FS2(T) (fig. 11(b)). (Note that several situations might result in a scan point being coded BA as shown in table I.) Thus, the plot of FS2(F) is abnormal and leads to abnormally low reflection and attenuation coefficients (below user-specified limits), which if left unfiltered would result in invalid reflection and attenuation coefficient images. In this example, locations where points were coded BA were filtered out; i.e., they had their ultrasonic property versus frequency plots set equal to the previous “good” scan point. This is the reason that the ultrasonic property versus frequency plots on the waveform display, as well as the image locations on the image display, do not appear abnormal. Thus, PSIDD allows the user to determine whether filtering is indeed necessary for the coded points and to review the actual digitization. Figure 7 also shows several points coded BV, including the scan location $x = 15, y = 17$ (fig. 11(c)). This situation results when the B1(T) waveform is improperly digitized at a lower amplitude setting than for the B2(T) waveform (note the respective voltage/division [V/D] settings) (table I and fig. 11(d)). Thus, the plot of B1(F) magnitude is grossly abnormal. Obviously, this situation is incorrect and points coded BV are filtered out and subsequently examined with PSIDD to look at the actual digitization.

b. Examination of waveforms and frequency-dependent properties at different regions of SiC/CAS composite plate

In this example, a rectangular SiC/CAS composite plate was contact scanned and the cross-correlation velocity image recalled in PSIDD (fig. 12(a)). This image shows low velocity regions in the upper left and lower right corners of the image that correspond to porosity clusters. It is of interest to investigate the differences at the high and low velocity regions. Moving the cursor to a high velocity scan location ($x = 14, y = 12$) at the center of the image (fig. 12(b)) and a low velocity scan location ($x = 2, y = 12$) at the upper left corner of the image (fig. 12(d)), respectively, the waveforms and ultrasonic properties versus frequency behavior can be compared

(figs. 12(c) and (e)). For the low velocity location, the back surface echoes B1(T) and B2(T) are clearly shifted to the right (out in time) (B2(T) is shifted most severely) in comparison to those for the high velocity spot. Thus, observed cross-correlation (pulse) velocity differences between the two regions are verified by examining the digitized waveforms (see respective information boxes at lower right of waveform displays). Further significant differences between the two locations are seen in the phase velocity versus frequency and attenuation coefficient versus frequency plots. For the low velocity location, phase velocity decreases with frequency while at the high velocity location, phase velocity increases with frequency. The slope of the attenuation coefficient versus frequency plot is significantly greater at the low velocity location than at the high velocity location.

After the attenuation coefficient image at 6 MHz for the SiC/CAS plate (fig. 13(a)) is retrieved, the video cursor is placed on a high attenuation coefficient location to examine the waveforms at that point (fig. 13(b)). In comparison to the waveforms at a low attenuation coefficient location (which is also a high velocity location) (fig. 12(c)), it is seen that B1(T) and B2(T) are highly attenuated and distorted. This manifests itself in oscillating and distorted B1(F) and B2(F) magnitude spectra and an oscillating attenuation coefficient versus frequency behavior with much greater attenuation coefficient values than those displayed at the low attenuation coefficient location. Figure 13(c) shows that B2(T) at this scan location retains the same distorted characteristic with or without system noise subtracted.

The velocity and attenuation coefficient images of the SiC/CAS composite reveal features similar to those seen in conventional x-ray and ultrasonic c-scan images of the composite;² however, PSIDD affords the opportunity to more closely examine the interaction of defects with ultrasound. As for the previous example showing the silicon nitride disk, it is envisioned that different material conditions in the composite (pore clusters, excess second phases, etc.) would generate characteristic signatures that could be identified through the combination of waveform shape and ultrasonic property versus frequency behavior.

V. Conclusion

An ultrasonic data display system was developed that allows the user to interactively examine digitized and processed information associated with any specific scan location of an ultrasonic contact scan. This information is displayed on a video display monitor and includes acquired time-domain waveforms, frequency-domain magnitude and phase spectra, and ultrasonic properties (pulse velocity, phase velocity, reflection coefficient, attenuation coefficient, attenuation coefficient error) as a function of frequency for a material. This report describes the system features and illustrates its usefulness for

nondestructive materials characterization. This system can serve as a component of an artificial intelligence system for automatic defect classification based on wave shape and ultrasonic property versus frequency characteristics. Additionally, PSIDD can be modified for use with immersion c-scanning where RF waveforms are digitized and stored. Other features such as display of waveforms with and without diffraction corrections can easily be added.

Lewis Research Center
National Aeronautics and Space Administration
Cleveland, Ohio, November 1993

VI. Appendix – Equations Used to Calculate Ultrasonic Properties

The following equations are valid for the pulse-echo configuration (fig. 1). Cross-correlation velocity is calculated from⁴

$$V = 2 \frac{X}{\tau_o} \quad (1)$$

where τ_o is the time shift for which

$$\left| \lim_{T \rightarrow \infty} \int_{-T}^T B_I(t) \odot B_2(t + \tau) \right| - \infty \leq \tau \leq \infty \quad (2)$$

reaches a maximum value and X is sample thickness.

Ultrasonic reflection coefficient is calculated according to⁵

$$|R(f)| = \left| \frac{FS_2(f)}{FS_1(f)} \right| \quad (3)$$

where f is frequency and $|FS_1(f)|$ and $|FS_2(f)|$ are the Fourier magnitude spectra of the time domain pulses $FS_1(t)$ and $FS_2(t)$ without and with the sample present on the buffer rod, respectively.

Attenuation coefficient is calculated according to⁵

$$\alpha(f) = \frac{1}{2X} \ln \frac{|B_1(f)| |R(f)|}{|B_2(f)|} \quad (4)$$

where $|B_1(f)|$ and $|B_2(f)|$ are the Fourier magnitude spectra of time-domain pulses $B_1(t)$ and $B_2(t)$, respectively. Percent error in the attenuation coefficient is calculated according to

$$\begin{aligned} \%ERR_{\alpha} \left(\frac{\sigma_{\alpha}}{\alpha} \right) 100 &= 100 \left(\frac{1}{2X\alpha} \right) \left(\frac{1}{SNR} \right) \\ &\times \left[\left(\frac{[\exp(4X\alpha)] [R^2 + \exp(4X\alpha)]}{(1 - R^2)^2} + 1 \right) \left(\frac{1}{R^2} \right) \right. \\ &\quad \left. + 1 + (SNR^2) (4\alpha^2) (\sigma_X^2) \right]^{0.5} \end{aligned} \quad (5)$$

where σ_{α} is the error in the attenuation coefficient measurement, X the sample thickness, σ_X the error in the thickness measurement, R the reflection coefficient, and SNR the signal-to-noise ratio.

Phase velocity is calculated according to⁶

$$V(f) = \frac{(2X)2\pi f}{\Delta\theta}, \quad \Delta\theta = \theta_1 - \theta_2 \quad (6)$$

where

$$\theta_1(f) = \tan^{-1} \frac{\text{Im}(B_I(f))}{\text{Re}(B_I(f))} \quad (7)$$

and

$$\theta_2(f) = \tan^{-1} \frac{\text{Im}(B_2(f))}{\text{Re}(B_2(f))} \quad (8)$$

where f is frequency and $B_1(f)$ and $B_2(f)$ are the Fourier transformations of time domain pulses $B_1(t)$ and $B_2(t)$, respectively.

VII. References

1. Roth, D.J., et al.: Quantitative Mapping of Pore Fraction Variations in Silicon Nitride Using an Ultrasonic Contact Scan Technique. NASA TP-3377.
2. Roth, D.J., et al.; NDE Approaches for Characterization of Microstructural Variations in Ceramic and Metal Matrix Composites. HITEMP Review 1993, Oct. 28-29, 1993, Cleveland, OH.
3. Grinnell Systems GMR Series Software Package User's Manual. Release 2.2, June 19, 1981, available from Mark McLoud Associates, 165-F Criflich Lane, Campbell, CA 95008, (Ph: 408-559-7888).
4. Hull, D.R.; Kautz, H.E.; and Vary, A.: Measurement of Ultrasonic Velocity Using Phase-Slope and Cross-Correlation Methods. Mater. Eval., vol. 43, no. 11, 1985, pp. 1455-1460.
5. Generazio, E.R., The Role of the Reflection Coefficient in Precision Measurement of Ultrasonic Attenuation. Materials Evaluation, Vol. 43, No. 8, 1985, pp. 995-1004.
6. Sachse, W.; and Pao, Y.H.: On the Determination of Phase and Group Velocities of Dispersive Waves in Solids. J. Appl. Phys, vol. 49, no. 8, 1978, pp. 4320-4327.

Table I.-Criteria for "Coding" Locations in Ultrasonic Contact Scan Images

Code and definition	Condition
BA - questionable attenuation coefficient values	Reflection coefficient at transducer center frequency is above or below user-specified limits. ^a Attenuation coefficient at transducer center frequency is above or below user specified limits. Fourier magnitude spectra of second back surface pulse B2(F) exhibits "significant" double-peak characteristic.
BC ^b - questionable cross-correlation velocity value	Cross-correlation velocity is above or below user-specified limits.
BE ^{b,c} - questionable data at edge locations	The first and last two locations in a scan row for irregularly shaped (egs. circular) sample.
BP ^b - questionable phase velocity values	Phase velocity at transducer center frequency is above or below user-specified limits.
BV ^b - questionable cross-correlation and phase velocity data	First back surface pulse B1(T) is improperly digitized at a lower amplitude setting than for the second back surface pulse B2(T).

^aQuestionable reflection coefficient will lead to a questionable attenuation coefficient.

^bPoints coded BC, BP, BV, or BE are implied to also be coded BA since any questionable waveform of the three acquired at a scan location will affect the attenuation coefficient calculation.

^cWhen the ultrasonic transducer is located at the interface between the edges of an irregularly shaped sample, such as a circular puck and the sample holder during an ultrasonic contact scan, scattering effects may take place making the waveforms of questionable validity.

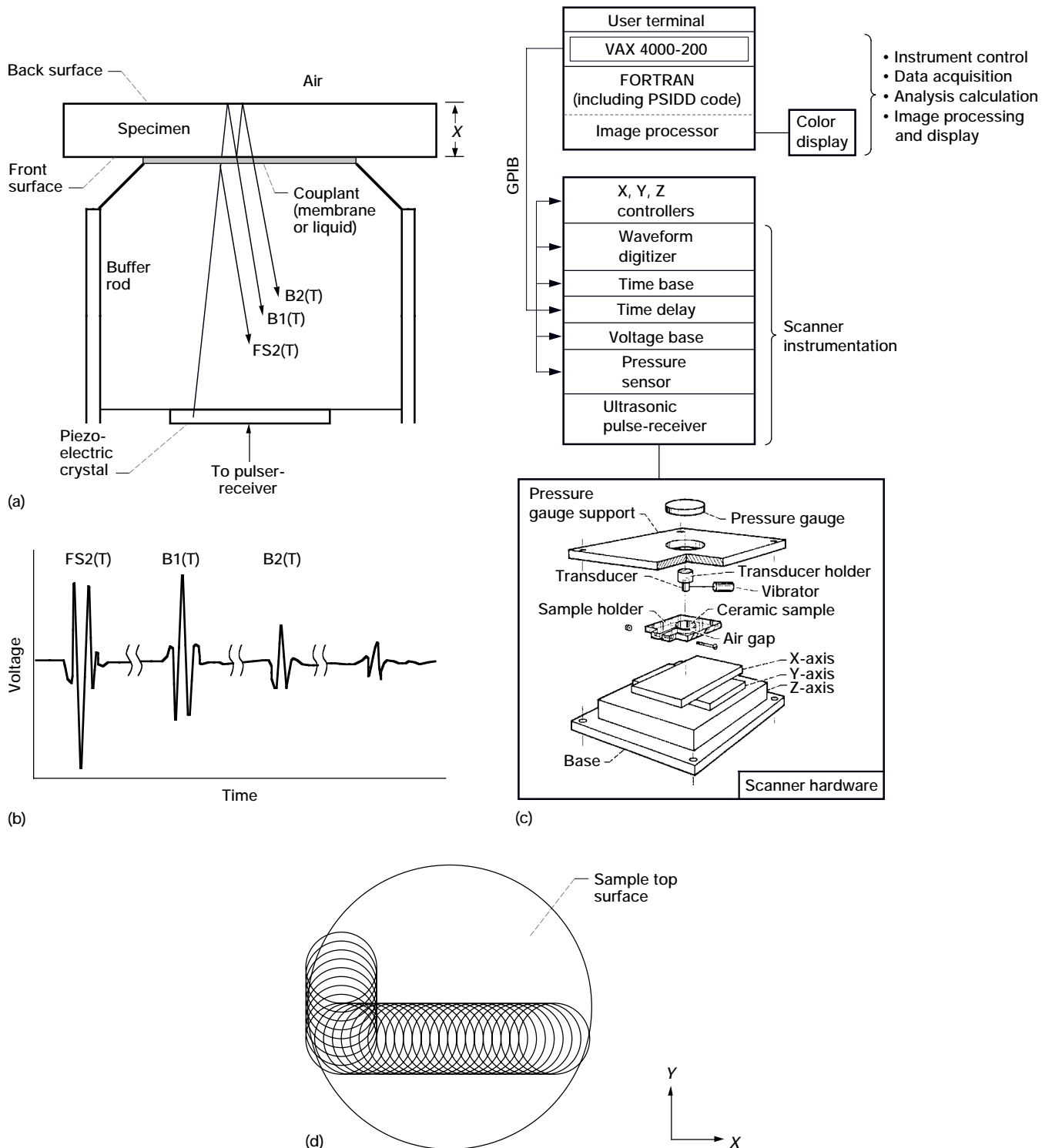
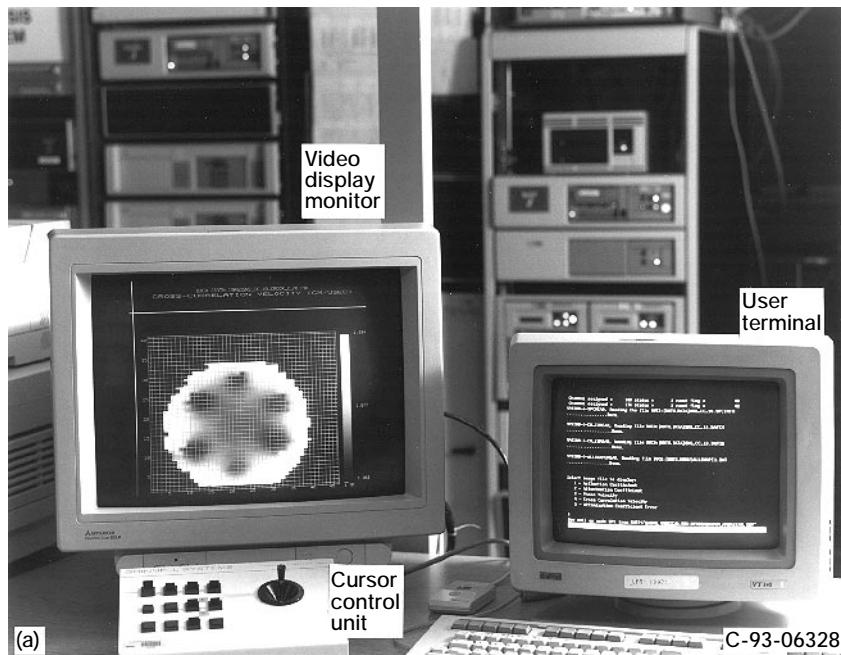


Figure 1.—Ultrasonic measurement method and contact scan system. (a) Diagram of buffer rod-couplant-sample pulse-echo contact configuration. $FS2(T)$ = front surface reflection; $B1(T)$ = first back-surface reflection; $B2(T)$ = second back-surface reflection. $FS1(T)$, not shown in this figure but shown in upcoming waveform displays, is acquired without sample or couplant on buffer rod. (b) Resulting waveforms for pulse-echo contact technique. (c) Computer-controlled ultrasonic contact scan system. (d) Schematic (top view) of ultrasonic contact scan procedure showing examples of successive transducer positions along X- and Y-dimensions of sample.



```

DON_SPR>RUN PSIDD
%PSIDD-I-START, PSIDD starting...

%PSIDD-I-INIREAD, Reading initialization file PSIDD.INI
.....Done.

%PSIDD-I-DADQREAD, Reading file DUC2:[ROTH.MENU]DADQ1.DAT
.....Done.

%PSIDD-I-DATASET, You will be working with the SN2_CC_10 datasets...
Do you wish to continue?

Y
GRINNELL IS AVAILABLE !
Channel assigned = 160 status = 1 event flag = 63
Channel assigned = 176 status = 1 event flag = 62
%PSIDD-I-SPCREAD, Reading the file DUCO:[ROTH.DATA]SN2_CC_10.SPCINFO
.....Done.

%PSIDD-I-CH_I2READ, Reading the file DUCO:[ROTH.DATA]SN2_CC_10.DATCH
.....Done.

%PSIDD-I-CH_I2READ, Reading the file DUCO:[ROTH.DATA]SN2_CC_10.DATI2
.....Done.

%PSIDD-I-ALLSHAPEREAD, Reading the file DUC2:[ROTH.MENU]ALLSHAPE1.DAT
.....Done.
(b)

```

```

Select image file to display:
1 - Reflection Coefficient
2 - Attenuation Coefficient
3 - Phase Velocity
4 - Cross Correlation Velocity
5 - Attenuation Coefficient Error

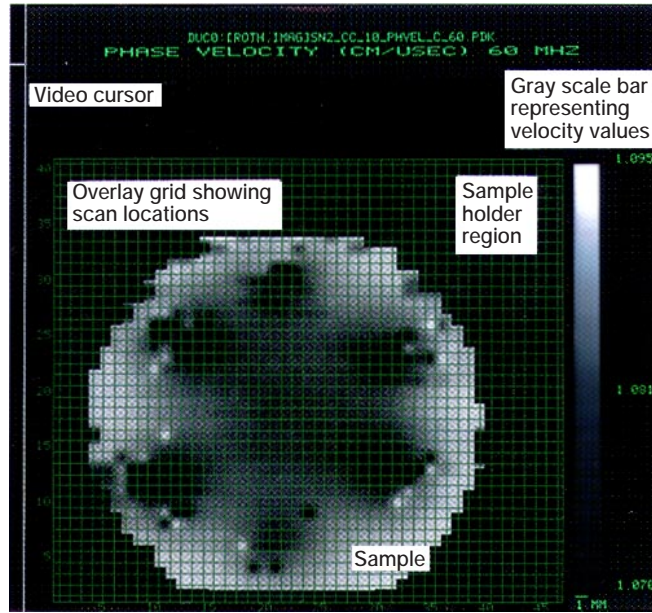
3

Select image frequency:
0 - 70MHz
1 - 40MHz
2 - 50MHz
3 - 60MHz
4 - 70MHz
5 - 80MHz
6 - 90MHz
7 - 100MHz
8 - 110MHz
9 - 120MHz

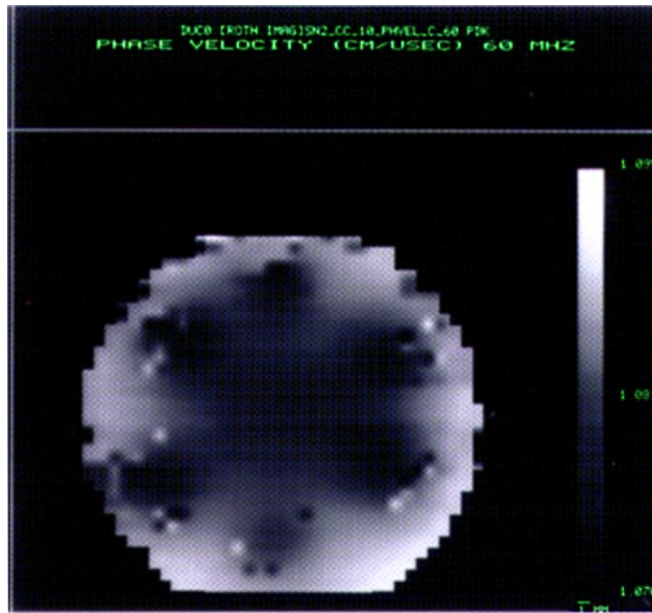
3
(c)

```

Figure 2.—Video display setup, queries to user and messages to user for PSIDD operation. (a) Video display setup. (b) Initial query and messages to user terminal. (c) Queries concerning image type and frequency to user terminal.



(a)



(b)

Figure 3.—Ultrasonic image (phase velocity, 60 MHz) of silicon nitride disk. (a) Image with superimposed grid showing locations of ultra-sonic measurements. (b) Image without superimposed grid.

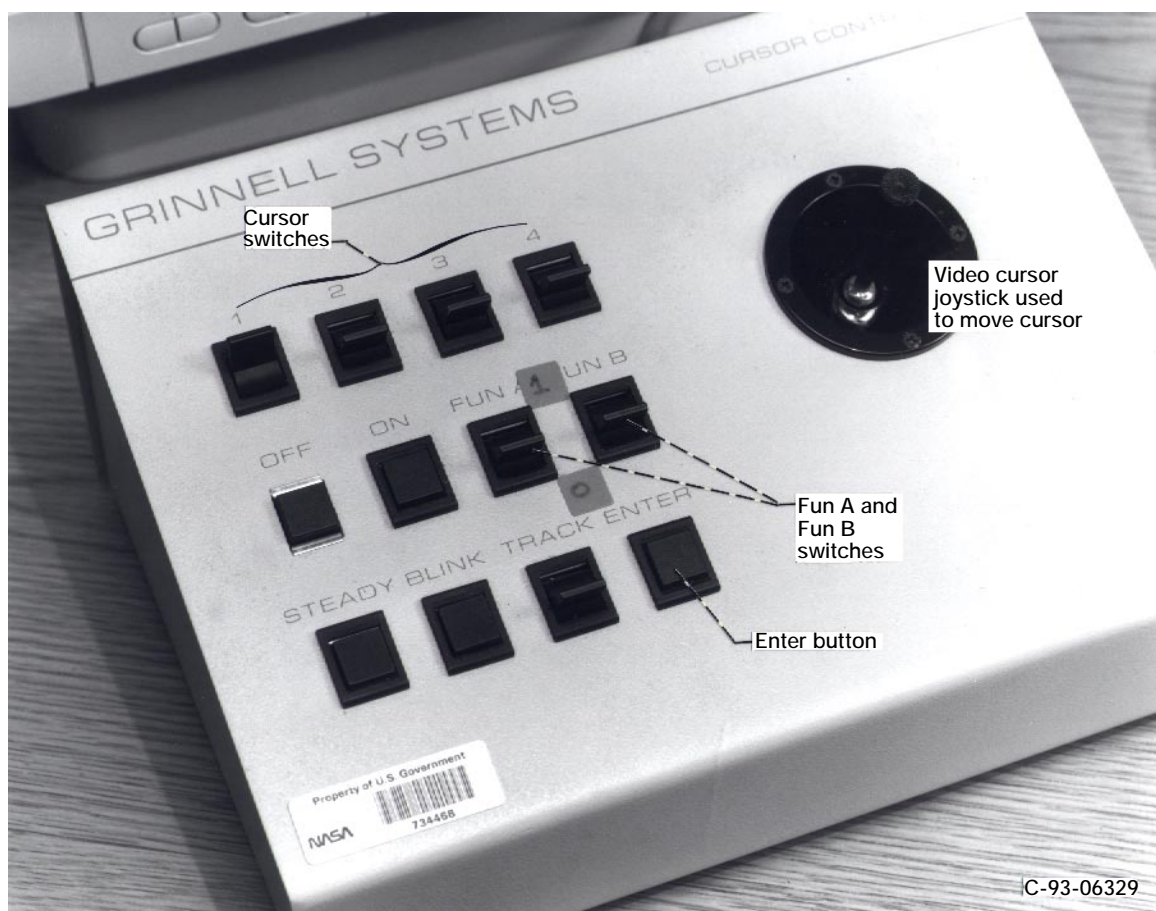


Figure 4.—Cursor control unit attached to image processing system.

Image Display Menu

FUN A	FUN B	Action to be performed when Enter is pressed on the Cursor Control Unit
0	0	If the cursor is on the image then display the waveform data corresponding to the cursor location on the image; otherwise toggle the image grid on and off.
0	1	Toggle the image display color scheme.
1	0	Toggle the display of the good/bad data on the image display.
1	1	Select a new image file to display.

(a)

Waveform Display Menu

FUN A	FUN B	Action to be performed when Enter is pressed on the Cursor Control Unit
0	0	Return to the image display.
0	1	Toggle the waveform display background color between black and white.
1	0	If the cursor is on one of the two back surface waveforms then the noise subtraction option is toggled. If the cursor is on one of the spectra graphs then the interpolation method is toggled between linear and spline.
1	1	Displays the graph underneath the waveform cursor on the graph display; i.e.enlarges the graph.

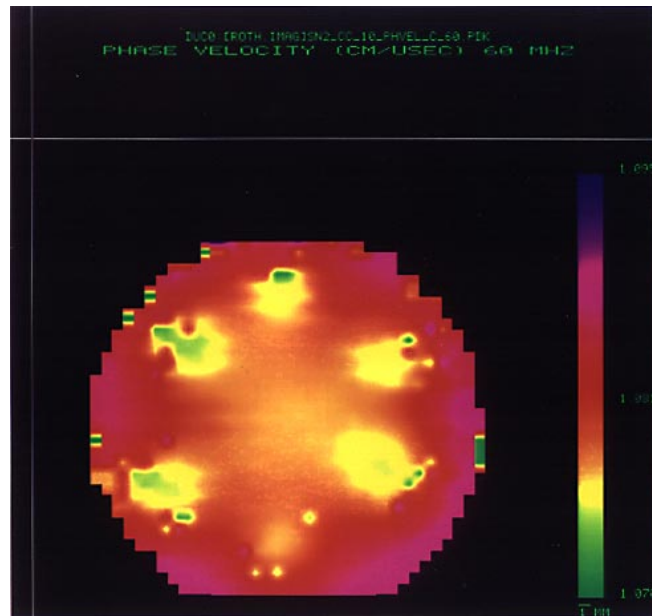
(b)

Graph Display Menu

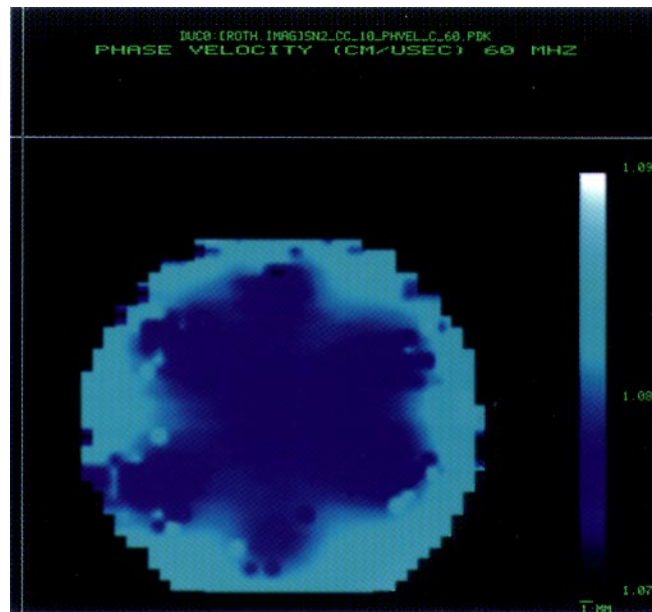
FUN A	FUN B	Action to be performed when Enter is pressed on the Cursor Control Unit
0	0	Return to the waveform display.
0	1	Toggle the graph display background color between black and white.
1	0	If the graph displayed is on one of the two back surface waveforms then the noise subtraction option is toggled. If the graph displayed is on one of the spectra graphs then the interpolation method is toggled between linear and spline.
1	1	If the graph display is one of one the two back surface waveforms then either the same waveform is overlayed with or without noise subtraction depending on the waveform currently displayed. If the graph display one of the spectra arrays then the same graph is overlayed with the other interpolation method.

(c)

Figure 5.—PSIDD cursor control: menus used in conjunction with cursor control unit for selecting options in PSIDD.
(a) Image display. (b) Waveform display. (c) Graph display.



(a)



(b)

Figure 6.—Example color schemes for ultrasonic contact scan images. (a) Example color scheme for image. (b) Example color scheme for image.

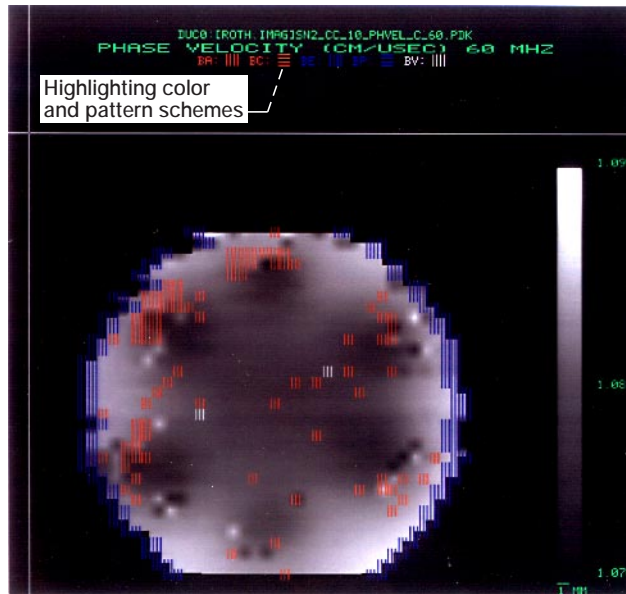
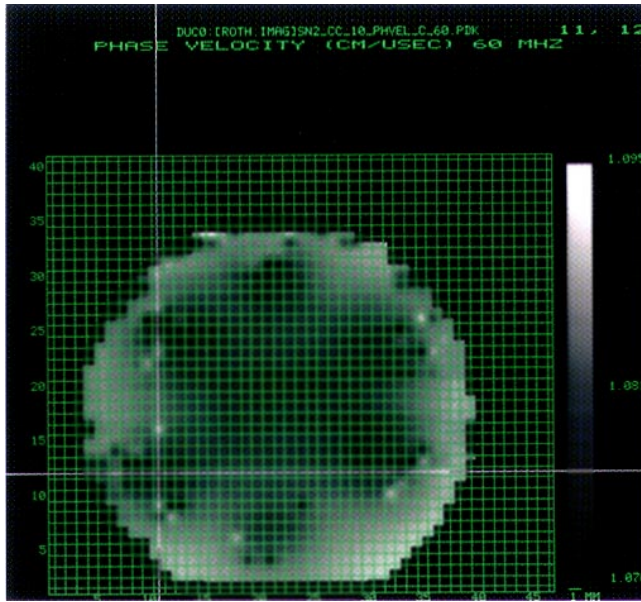
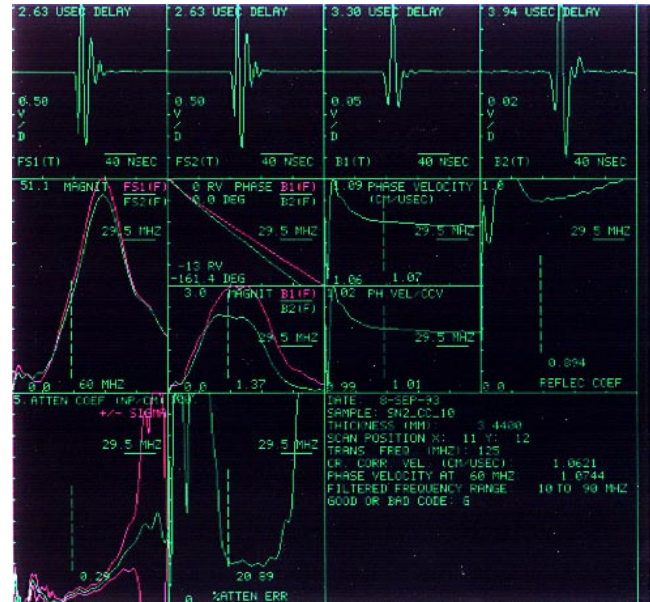


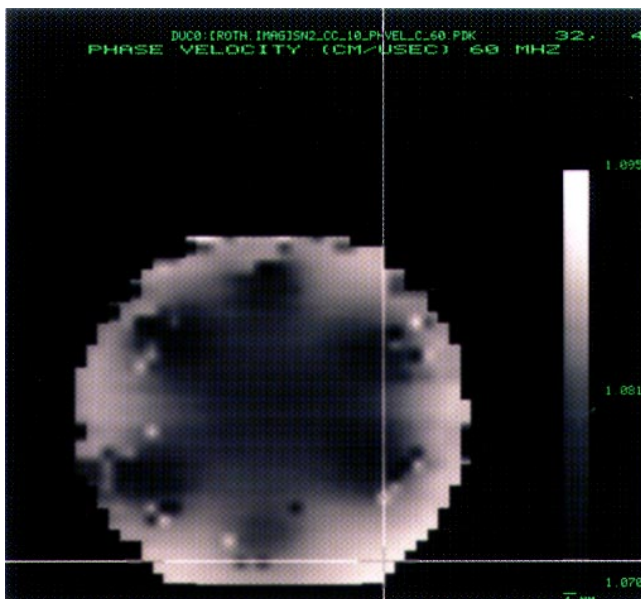
Figure 7.—Ultrasonic image (phase velocity, 60 MHz) with high-lighted scan locations representing locations of questionable data.



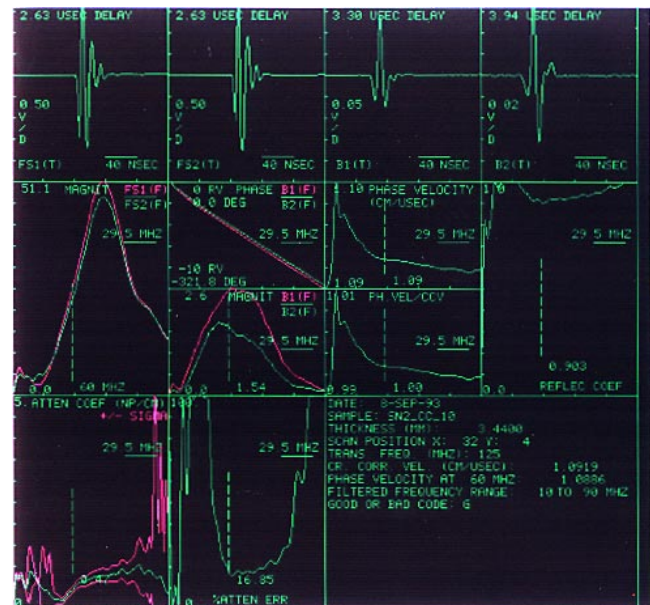
(a)



(b)

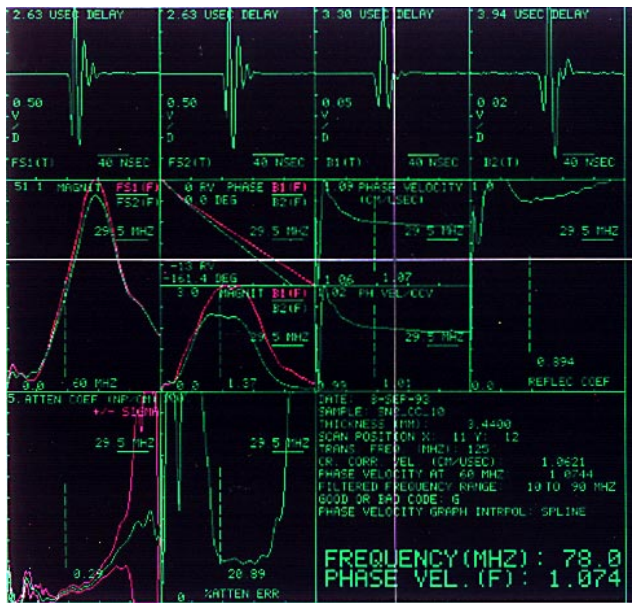


(c)



(d)

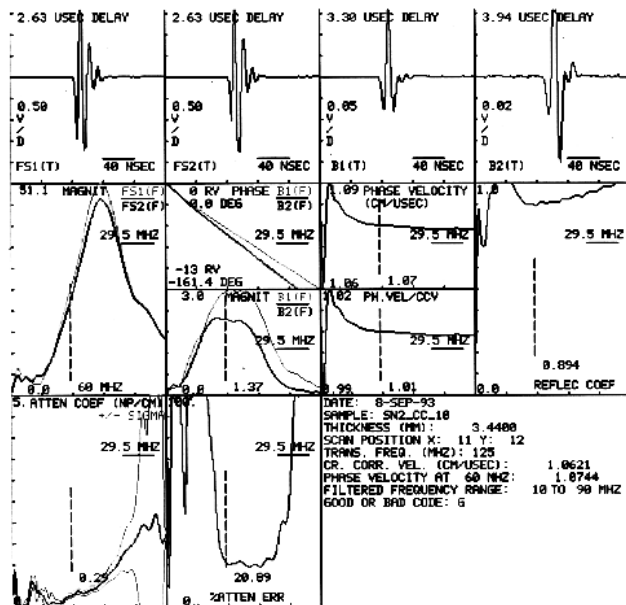
Figure 8.—Moving video cursor to different locations in ultrasonic (phase velocity, 60 MHz) image to obtain waveform display at those locations. (a) Video cursor moved to scan location ($x = 11$, $y = 12$) of dark color (low velocity). (b) Waveform display for scan location $x = 11$, $y = 12$. (c) Video cursor moved to scan location ($x = 32$, $y = 4$) of light color (high velocity). (d) Waveform display for scan location $x = 32$, $y = 4$.



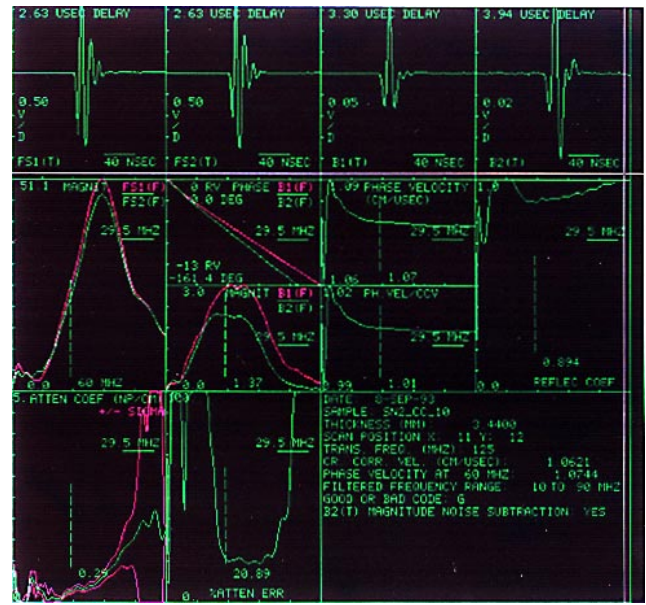
(e)



(f)



(g)

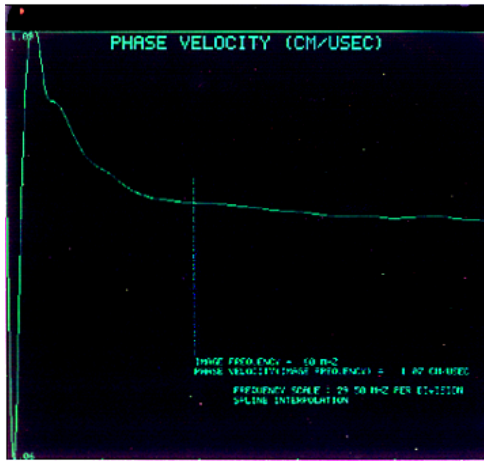


(h)

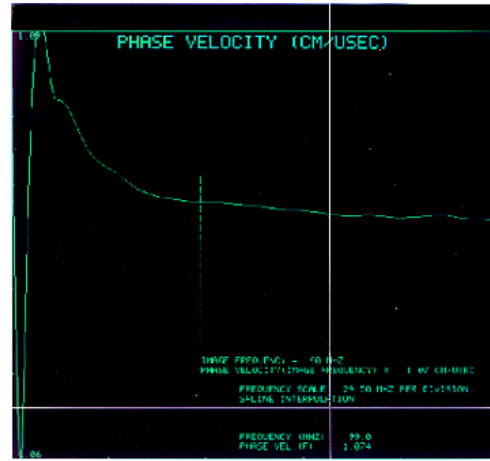
Figure 8.—Concluded. (e) Moving video cursor in phase velocity box of waveform display allows display of phase velocity at any frequency. (f) Moving video cursor in B1(F)/B2(F) magnitude box of waveform display allows display of ratio B1(F)/B2(F) at any frequency. (g) Gray scale color scheme for waveform display. (h) With video cursor in B2(T) box, noise originally present without sample on buffer rod (fig. 1) can be subtracted.



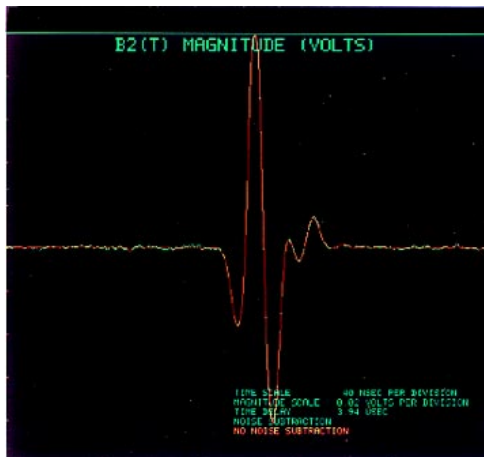
(a)



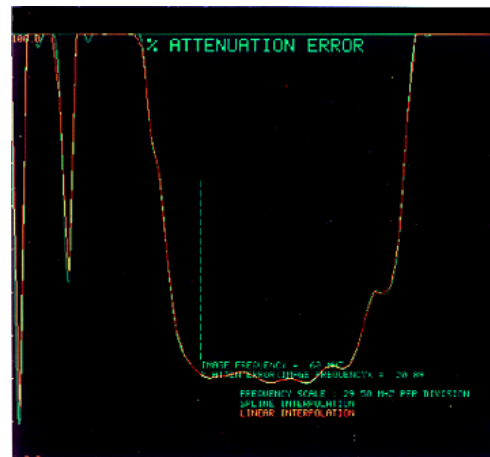
(b)



(c)

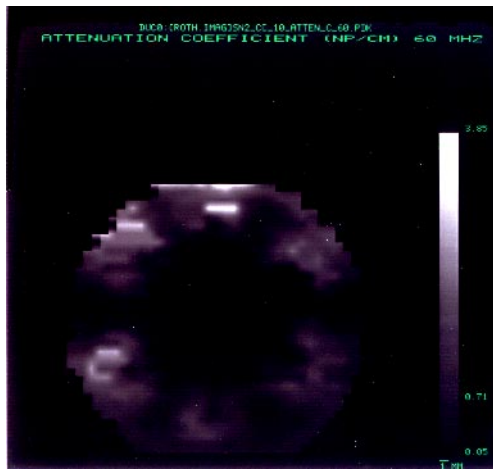


(d)

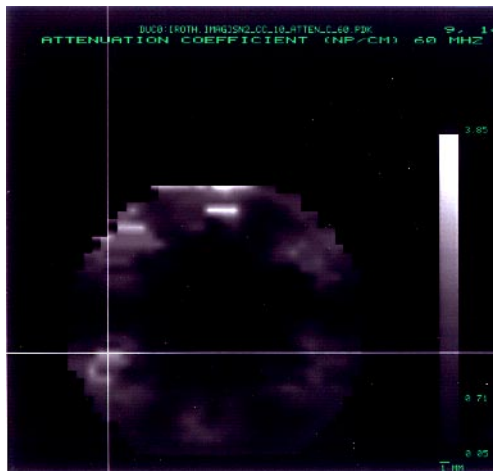


(e)

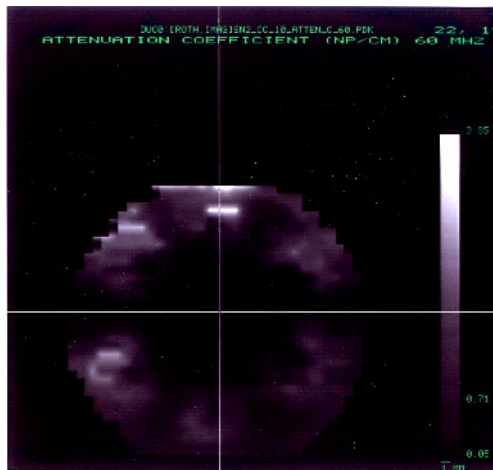
Figure 9.—Enlarged displays at scan location $x = 11$, $y = 12$. (a) Enlarged display of waveform B2(T). (b) Enlarged display of phase velocity graph. (c) Enlarged display with interactive video cursor allowing display of ultrasonic property at any frequency. (d) B2(T) waveform with noise subtracted (green) and without noise subtracted (orange). Not much difference is noted between the two in this example. (e) Percent attenuation coefficient error with spline (green) and linear (orange) interpolation options overlaid.



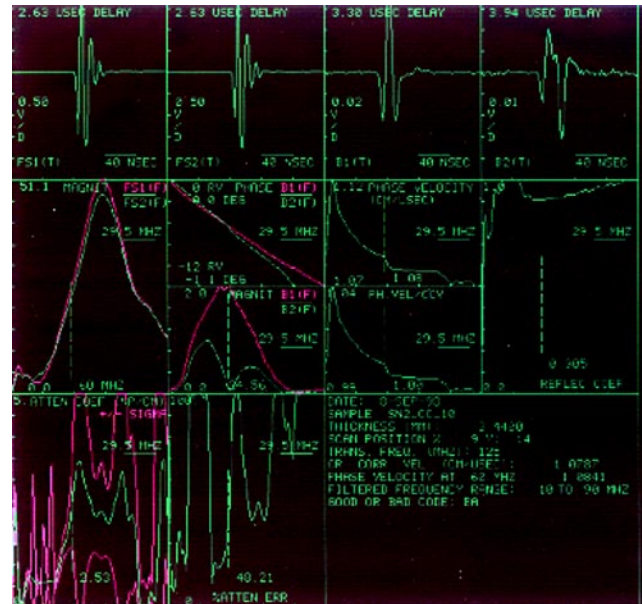
(a)



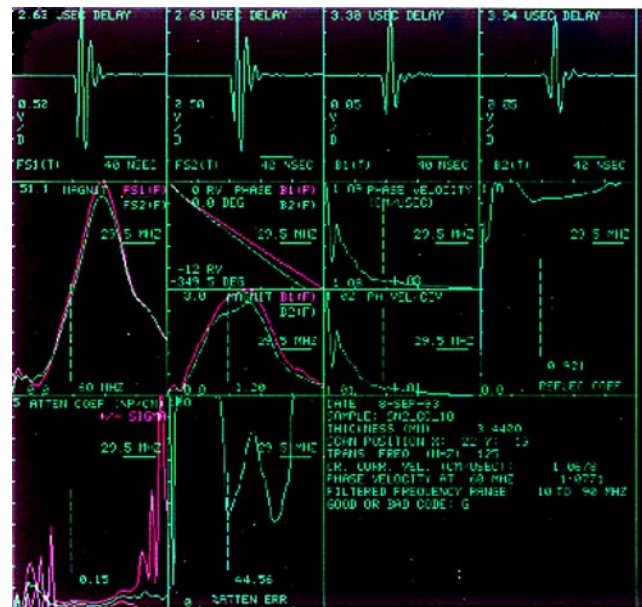
(b)



(d)

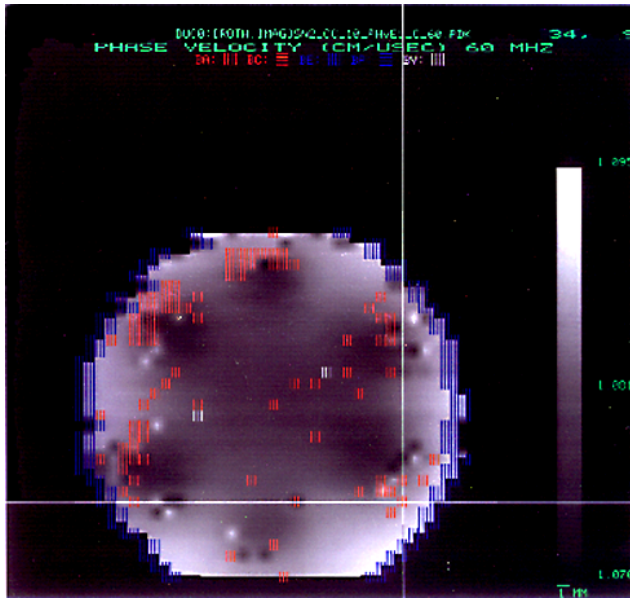


(c)

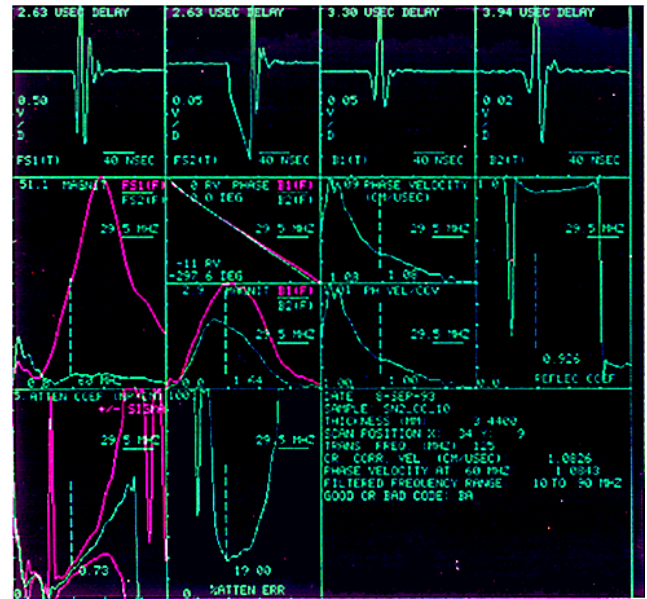


(e)

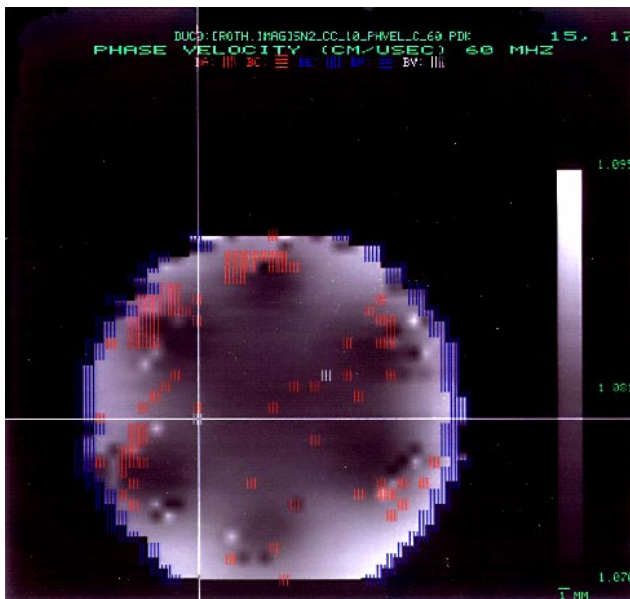
Figure 10.—Attenuation coefficient image of silicon nitride disk and movement of video cursor to different locations in image to obtain waveform display at those locations. (a) Attenuation coefficient (60 MHz) image. (b) Video cursor moved to scan location (x = 9, y = 14) of light color (high attenuation coefficient) corresponding to edge of dark region seen in phase velocity (60 MHz) image (fig. 8). (c) Waveform display for scan location x = 9, y = 14. (d) Video cursor moved to scan location (x = 22, y = 9) of dark color (low attenuation coefficient). (e) Waveform display for scan location x = 22, y = 19.



(a)



(b)



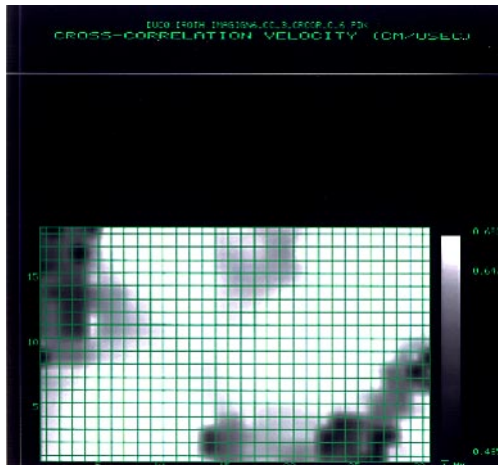
(c)



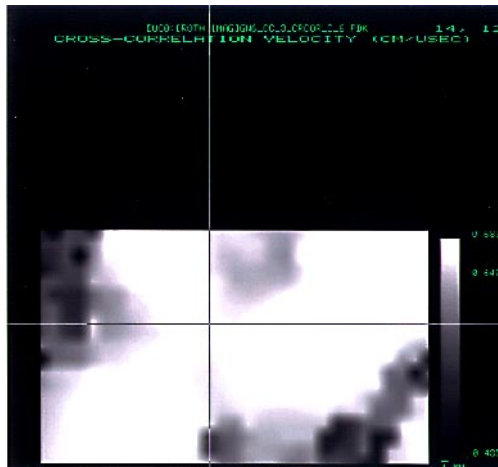
(d)

Figure 11.—Waveform displays for coded points of ultrasonic (phase velocity, 60 MHz) image of silicon nitride disk.

- (a) Video cursor moved to scan location (x = 34, y = 9) coded BA. (b) Waveform display for scan location x = 34, y = 9.
(c) Video cursor moved to scan location (x = 15, y = 17) coded BV. (d) Waveform display for scan location x = 15, y = 17.



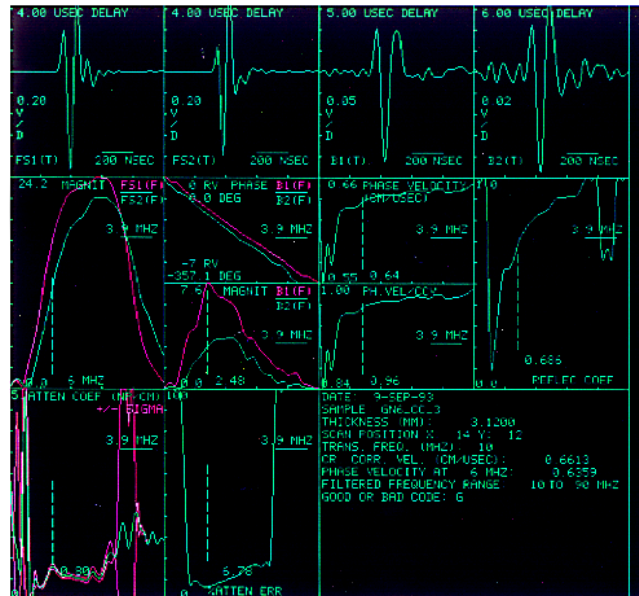
(a)



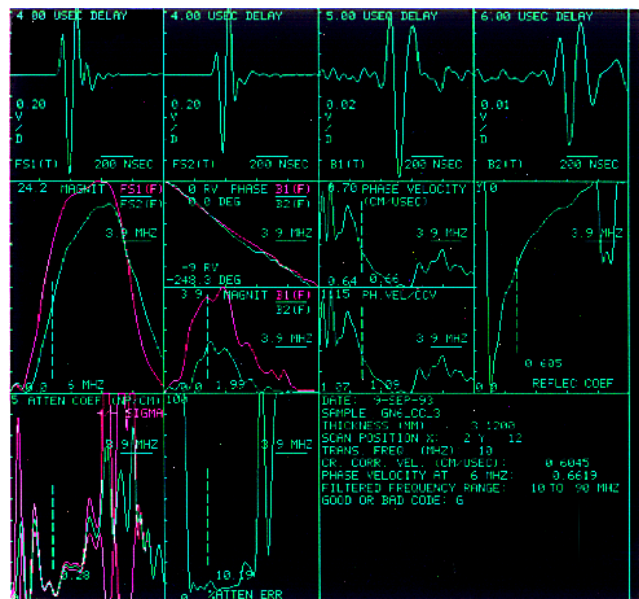
(b)



(d)

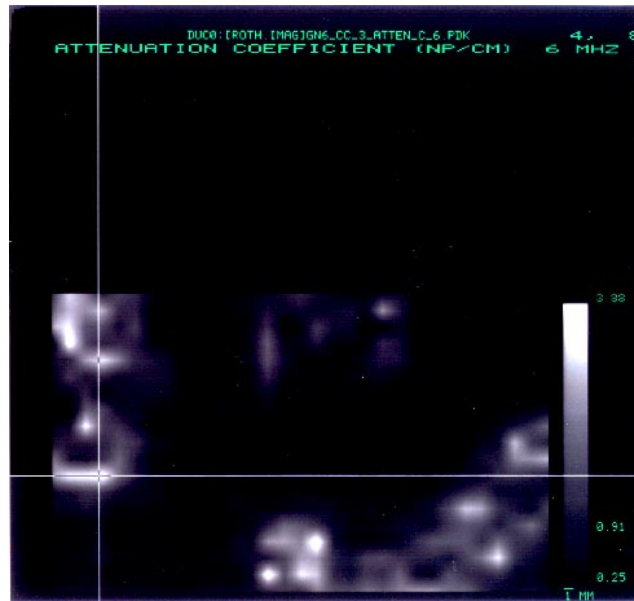


(c)

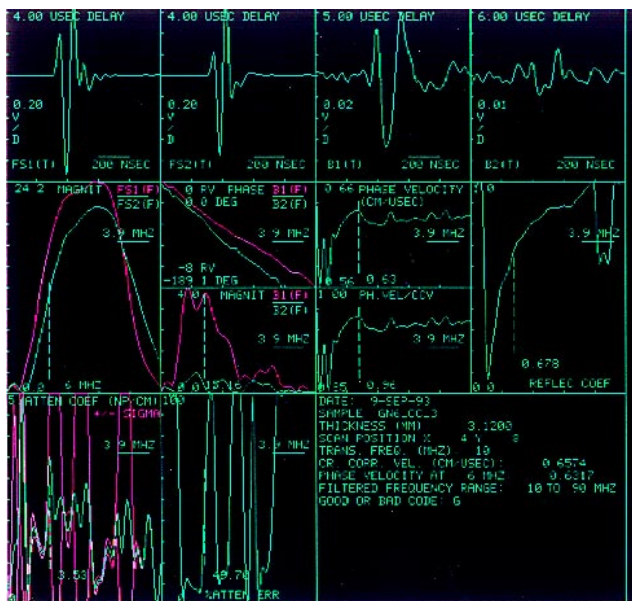


(e)

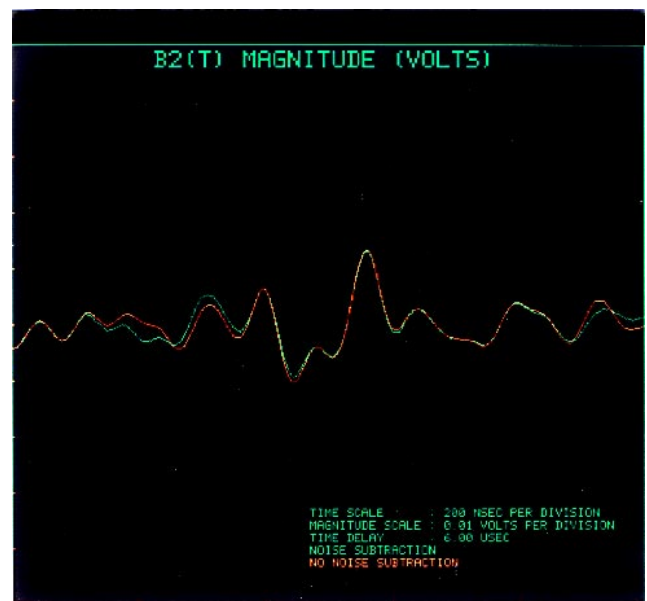
Figure 12.—Ultrasonic (cross-correlation) velocity image of SiC/CAS plate and movement of video cursor to different locations in image to obtain waveform display at those location. (a) Image with superimposed grid showing locations of ultrasonic measurements. (b) Video cursor moved to scan location (x = 14, y = 12) of light color (high velocity). (c) Waveform display for scan location x = 14, y = 12. (d) Video cursor moved to scan location (x = 2, y = 12) of dark color (low velocity). (e) Waveform display for scan location x = 2, y = 12.



(a)



(b)



(c)

Figure 13.—Ultrasonic (attenuation coefficient, 60 MHz) image of SiC/CAS plate and movement of video cursor to high attenuation coefficient location. (a) Video cursor moved to scan location (x = 4, y = 8) of light color (high attenuation coefficient). (b) Waveform display for scan location x = 4, y = 8. (c) Enlarged display of B2(T) magnitude graph showing waveform with noise subtracted (green) and without noise subtracted (orange).

REPORT DOCUMENTATION PAGE			Form Approved OMB No. 0704-0188	
Public reporting burden for this collection of information is estimated to average 1 hour per response, including the time for reviewing instructions, searching existing data sources, gathering and maintaining the data needed, and completing and reviewing the collection of information. Send comments regarding this burden estimate or any other aspect of this collection of information, including suggestions for reducing this burden, to Washington Headquarters Services, Directorate for Information Operations and Reports, 1215 Jefferson Davis Highway, Suite 1204, Arlington, VA 22202-4302, and to the Office of Management and Budget, Paperwork Reduction Project (0704-0188), Washington, DC 20503.				
1. AGENCY USE ONLY (Leave blank)	2. REPORT DATE November 1993	3. REPORT TYPE AND DATES COVERED Technical Memorandum		
4. TITLE AND SUBTITLE PSIDD: A Post-Scan Interactive Display System for Ultrasonic Scans		5. FUNDING NUMBERS WU-510-01-50		
6. AUTHOR(S) Don J. Roth and Steven A. Szatmary				
7. PERFORMING ORGANIZATION NAME(S) AND ADDRESS(ES) National Aeronautics and Space Administration Lewis Research Center Cleveland, Ohio 44135-3191		8. PERFORMING ORGANIZATION REPORT NUMBER E-8167		
9. SPONSORING/MONITORING AGENCY NAME(S) AND ADDRESS(ES) National Aeronautics and Space Administration Washington, DC 20546-0001		10. SPONSORING/MONITORING AGENCY REPORT NUMBER NASA TM-4545		
11. SUPPLEMENTARY NOTES Don J. Roth, NASA Lewis Research Center; and Steven A. Szatmary, Cleveland State University, 1983 East 24th Street, Cleveland, Ohio 44115. Responsible person, Don J. Roth, (216) 433-6017.				
12a. DISTRIBUTION/AVAILABILITY STATEMENT Unclassified - Unlimited Subject Category 38			12b. DISTRIBUTION CODE	
13. ABSTRACT (Maximum 200 words) An ultrasonic data display system was developed at NASA Lewis Research Center that allows the user to interactively examine digitized waveforms and processed information associated with any specific scan location of an ultrasonic contact scan. This information is displayed on a video display monitor and includes acquired time-domain waveforms, frequency-domain magnitude and phase spectra, and ultrasonic properties (pulse velocity, phase velocity, reflection coefficient, attenuation coefficient, attenuation coefficient error) as a function of frequency for a material. This report describes the system features and illustrates the system's usefulness for nondestructive materials characterization.				
14. SUBJECT TERMS Ultrasonics; Nondestructive testing; Signal analysis; Velocity; Attenuation; Image analysis			15. NUMBER OF PAGES 24	
			16. PRICE CODE A03	
17. SECURITY CLASSIFICATION OF REPORT Unclassified	18. SECURITY CLASSIFICATION OF THIS PAGE Unclassified	19. SECURITY CLASSIFICATION OF ABSTRACT Unclassified	20. LIMITATION OF ABSTRACT	